JOURNAL OF THE AERONAUTICAL SCIENCES

SUBSCRIPTION RATES

Journal of the Aeronautical Sciences, Published Monthly.—United States and Possessions: 1 Year, $15.00; Single Copies, $1.50. Foreign Countries Including Canada (American Currency Rates): 1 Year, $16.00; Single Copies, $1.50.

Aeronautical Engineering Review, Published Monthly.—United States and Possessions: 1 Year, $3.00; Single Copies, $0.50. Foreign Countries Including Canada (American Currency Rates): 1 Year, $3.50; Single Copies, $0.50.

Notices of change of address should be sent to the Institute at least 30 days prior to actual change of address.

Manuscripts for publication, proofs, and all correspondence should be addressed to the Editorial Office of the Journal.

Correspondence regarding subscriptions may be addressed to the Editorial Office of the Journal of the Aeronautical Sciences, 2 East 64th Street, New York 21, N.Y., or to the Publication Office, 20th and Northampton Sts., Easton, Pa.

Entered as Second Class Matter at the Post Office, Easton, Pa., May 1, 1937. Acceptance for mailing at a special rate of Postage provided for in the Act of August 24, 1912. Authorized April 29, 1937.

JOURNAL OF THE AERONAUTICAL SCIENCES

VOLUME 23 SEPTEMBER, 1956 NUMBER 9

Stiffness and Deflection Analysis of Complex Structures

M. J. TURNER,* R. W. CLOUGH,† H. C. MARTIN,‡ AND L. J. TOPP**

ABSTRACT

A method is developed for calculating stiffness influence coefficients of complex shell-type structures. The object is to provide a method that will yield structural data of sufficient accuracy to be adequate for subsequent dynamic and aeroelastic analyses.

Stiffness of the complete structure is obtained by summing stiffnesses of individual units. Stiffnesses of typical structural components are derived in the paper. Basic conditions of continuity and equilibrium are established at selected points (nodes) in the structure. Increasing the number of nodes increases the accuracy of results. Any physically possible support conditions can be taken into account. Details in setting up the analysis can be performed by nonengineering trained personnel; calculations are conveniently carried out on automatic digital computing equipment.

Method is illustrated by application to a simple truss, a flat plate, and a box beam. Due to shear lag and spar web deflection, the box beam has a 25 per cent greater deflection than predicted from beam theory. It is shown that the proposed method correctly accounts for these effects.

Considerable extension of the material presented in the paper is possible.

(I) INTRODUCTION

PRESENT CONFIGURATION TRENDS in the design of high-speed aircraft have created a number of difficult, fundamental structural problems for the worker in aeroelasticity and structural dynamics. The chief problem in this category is to predict, for a given elastic structure, a comprehensive set of load-deflection relations which can serve as structural basis for dynamic load calculations, theoretical vibration and flutter analyses, estimation of the effects of structural deflection on static air loads, and theoretical analysis of aeroelastic effects on stability and control. This is a problem of exceptional difficulty when thin wings and tail surfaces of low aspect ratio, either swept or unswept, are involved.

It is recognized that camber bending (or rib bending) is a significant feature of the vibration modes of the newer configurations, even of the low-order modes; in order to encompass these characteristics it seems likely that the load-deflection relations of a practical structure must be expressed in the form of either deflection or stiffness influence coefficients. One approach is to employ structural models and to determine the influence coefficients experimentally; it is anticipated that the experimental method will be employed extensively in the future, either in lieu of or as a final check on the result of analysis. However, elaborate models are expensive, they take a long time to build, and tend to become obsolete because of design changes; for these reasons it is considered essential that a continuing research effort should be applied to the development of analytical methods. It is to be expected that modern developments in high-speed digital computing machines will make possible a more fundamental approach to the problems of structural analysis; we shall expect to base our analysis on a more realistic and detailed conceptual model of the real structure than has been used in the past. As indicated by the title, the present paper is exclusively concerned with methods of theoretical analysis; also it is our object to outline the development of a method that is well adapted to the use of high-speed digital computing machinery.

(II) REVIEW OF EXISTING METHODS OF STRUCTURAL ANALYSIS

(1) *Elementary Theories of Flexure and Torsion*

The limitations of these venerable theories are too well known to justify extensive comment. They are

Received June 29, 1955. This paper is based on a paper presented at the Aeroelasticity Session, Twenty-Second Annual Meeting, IAS, New York, January 25–29, 1954.

* Structural Dynamics Unit Chief, Boeing Airplane Company, Seattle Division.

† Associate Professor of Civil Engineering, University of California, Berkeley.

‡ Professor of Aeronautical Engineering, University of Washington, Seattle.

** Structures Engineer, Structural Dynamics Unit, Boeing Airplane Company, Wichita Division.

adequate only for low-order modes of elongated structures. When the loading is complex (as in the case of inertia loading associated with a mode of high order) refinements are required to account for secondary effects such as shear lag and torsion-bending.

(2) ***Wide Beam Theory: Schuerch***[1]

Schuerch has devised a generalized theory of combined flexure and torsion which is applicable to multispar wide beams having essentially rigid ribs. Torsion-bending effects are included but not shear lag. It is expected that wide beam theory will be used extensively in the solution of static aeroelastic problems (effect of air-frame flexibility on steady air loads, stability, etc.). However, the rigid rib assumption appears to limit its utility rather severely for vibration and flutter analysis of thin low aspect ratio wings.

(3) ***Method of Redundant Forces: Levy, Bisplinghoff and Lang, Langefors, Rand, Wehle and Lansing***[2–6]

These writers have contributed the basic papers leading to the present widespread use of energy principles, matrix algebra, and influence coefficients in the solution of structural deflection problems. Redundant internal loads are determined by the principle of least work, and deflections are obtained by application of Castigliano's theorem. The method is, of course, perfectly general. However, the computational difficulties become severe if the structure is highly redundant, and the method is not particularly well adapted to the use of high-speed computing machines. Rand has suggested a method of solution for stresses in highly redundant structures which might also be used for calculating deflections. Instead of using member loads as redundants, he proposes to employ systems of self-equilibrating internal stresses. These redundant stresses may be regarded as perturbations of a primary stress distribution that is in equilibrium with the external loads (but does not generally satisfy compatibility conditions). The number of properly chosen redundants required to obtain a satisfactory solution may be considerably less than the "degree of redundancy." Successful application of this method requires a high degree of engineering judgment, and the accuracy of the results is very difficult to evaluate.

(4) ***Plate Methods: Fung, Reissner, Benscoter, and MacNeal***[7–9]

As the trend toward thinner sections approaches the ultimate limit, we enter first a regime of very thick walled hollow structures, such that the flexural and torsional rigidities of the individual walls make a significant contribution to the overall stiffness of the entire wing. Finally we come to the solid plate of variable thickness. During the past few years a substantial research effort has been devoted to the development of methods of deflection analysis for these structural types, and important contributions have been made by all of the aforementioned authors.

(5) ***Direct Stiffness Calculation: Levy, Schuerch***[10, 11]

In a recent paper Levy has presented a method of analysis for highly redundant structures which is particularly suited to the use of high-speed digital computing machines. The structure is regarded as an assemblage of beams (ribs and spars) and interspar torque cells. The stiffness matrix for the entire structure is computed by simple summation of the stiffness matrices of the elements of the structure. Finally, the matrix of deflection influence coefficients is obtained by inversion of the stiffness matrix. Schuerch has also presented a discussion of the problem from the point of view of determining the stiffness coefficients.

(III) Some Unsolved Problems

At the present time, it is believed that the greatest need is to derive a numerical method of analysis for a class of structures intermediate between the thin stiffened shell and the solid plate. These are hollow structures having a rather large share of the bending material located in the skin, which is relatively thick but still thin enough so that we may safely neglect its plate bending stiffness. In order to cope with this class of structures successfully, we must base our analysis upon a structural idealization that is sufficiently realistic to encompass a fairly general two-dimensional stress distribution in the cover plates; and our method of analysis must yield the load-deflection relations associated with such stresses. It is characteristic of these problems that the directions of principal stresses in certain critical parts of the structure cannot be determined by inspection. Hence, the familiar methods of structural analysis based upon the concepts of axial load carrying members, joined by membranes carrying pure shear, are not satisfactory, even if we employ effective width concepts to account for the bending resistance of the skin. We should like to include shear lag, torsion-bending, and Poisson's ratio effects to a sufficient approximation for reliable prediction of vibration modes and natural frequencies of moderate order. Also, we should like to avoid any assumptions of closely spaced rigid diaphragms or of orthotropic cover plates, which have been introduced in many papers on advanced structural analysis. The actual rib spacing and finite rib stiffnesses should be accounted for in a realistic fashion. In summary, what is required is an approximate numerical method of analysis which avoids drastic modification of the geometry of the structure or artificial constraints of its elastic elements. This is indeed a very large order. However, modern developments in high-speed digital computing machines offer considerable hope that these objectives can be attained.

(IV) Method of Direct Stiffness Calculation

For a given idealized structure, the analysis of stresses and deflections due to a given system of loads is a purely mathematical problem. Two conditions

must be satisfied in the analysis: (1) the forces developed in the members must be in equilibrium and (2) the deformations of the members must be compatible—i.e., consistent with each other and with the boundary conditions. In addition, the forces and deflections in each member must be related in accordance with the stress-strain relationship assumed for the material.

The analysis may be approached from two different points of view. In one case, the forces acting in the members of the structure are considered as unknown quantities. In a statically indeterminate structure, an infinite number of such force systems exist which will satisfy the equations of equilibrium. The correct force system is then selected by satisfying the conditions of compatible deformations in the members. This approach has been widely used for the analysis of all types of indeterminate structures but is, as already noted, particularly advantageous for structures that are not highly redundant.

In the other approach, the displacements of the joints in the structure are considered as unknown quantities. An infinite number of systems of mutually compatible deformations in the members are possible; the correct pattern of displacements is the one for which the equations of equilibrium are satisfied. The concept of static determinateness or indeterminateness is irrelevant when the analysis is considered from this viewpoint. This approach is the basis for many relaxation type analyses (such as moment distribution) and has been applied to the analysis of complex aircraft structures by Levy in the aforementioned paper. This will be called the method of direct stiffness calculation hereafter.

After reviewing the various methods available to the dynamics engineer for computing load-deflection relations of elastic structures, it is concluded that the most promising approach to our present difficulties is to extend further the method of direct stiffness calculation. The remainder of this paper is concerned with methods by which that extension may be accomplished.

(V) Simple Examples of Stiffness Influence Coefficients

(1) *Elastic Spring*

If an elastic spring deflects an amount δ under axial load F, Hooke's Law applies and

$$F = k\delta \tag{1}$$

Here k can be regarded as the force required to produce a unit deflection; hence it can be considered to be a stiffness influence coefficient.

Eq. (1) can also be written as

$$\delta = (1/k)F = cF \tag{2}$$

where c is the deflection due to a unit force (deflection influence coefficient).

(2) *Two-Dimensional Elastic Body*

Extending the above relations to the two-dimensional body is most conveniently accomplished by introducing

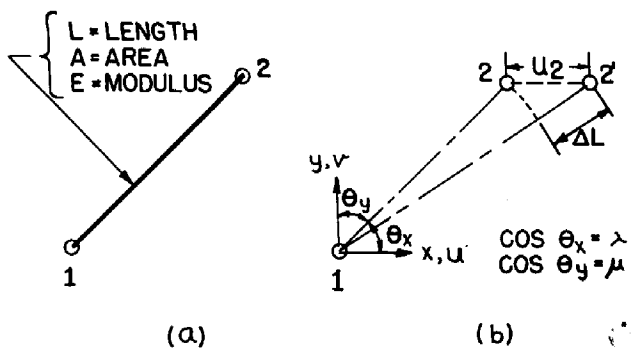

FIG. 1. Typical pin-ended truss member.

matrix notation. Eqs. (1) and (2) become, respectively,

$$\{F\} = [K]\{\delta\} \tag{3}$$

$$\{\delta\} = [K]^{-1}\{F\} = [C]\{F\} \tag{4}$$

Here $[K]$ is the matrix of stiffness influence coefficients. A typical element of $[K]$ is $k_{ij}^{\xi\eta}$ = force required at i in the ξ-direction, to support a unit displacement at j in the η-direction. If ξ and η always refer to the same direction, we can use the simpler form k_{ij}. In either case an element of $[K]$, and also of $[C]$, must obey the well-known reciprocal relations. In other words, the $[K]$ and $[C]$ matrices are symmetric, provided they are referred to orthogonal coordinate systems. As will be seen later, the symmetry condition does not apply if oblique coordinates are used.

(3) *Truss Member*

Fig. 1(a) shows a typical pin ended truss member. We wish to determine its matrix of stiffness influence coefficients. Loads may be applied at points (nodes) 1 and 2. Each node can experience two components of displacement. Therefore, prior to introducing boundary conditions (supports), $[K]$ for this member will be of order 4×4.

To develop one column of $[K]$, subject the member to $u_2 \neq 0$, $u_1 = v_1 = v_2 = 0$. Then

$$\Delta L = u_2 \cos\theta_x = u_2\lambda$$

The axial force needed to produce ΔL is

$$P = (AE/L)\Delta L = (AE/L)\lambda\, u_2$$

The components of P at node 2 are

$$F_{x_2} = P\cos\theta_x = (AE/L)\,\lambda^2\, u_2$$

$$F_{y_2} = P\cos\theta_y = (AE/L)\,\lambda\mu\, u_2$$

Equilibrium gives the forces at node 1 as

$$F_{x_1} = -F_{x_2}$$

$$F_{y_1} = -F_{y_2}$$

Eq. (3) for this member then takes the form

$$\begin{Bmatrix} F_{x_1} \\ F_{x_2} \\ F_{y_1} \\ F_{y_2} \end{Bmatrix} = \frac{AE}{L}\begin{bmatrix} \cdot & -\lambda^2 & \cdot & \cdot \\ \cdot & \lambda^2 & \cdot & \cdot \\ \cdot & -\lambda\mu & \cdot & \cdot \\ \cdot & \lambda\mu & \cdot & \cdot \end{bmatrix}\begin{Bmatrix} u_1 \\ u_2 \\ v_1 \\ v_2 \end{Bmatrix} \tag{5}$$

The other elements in $[K]$ are found in a similar manner. We get

$$[K]_{\substack{\text{truss}\\ \text{member}}} = \frac{AE}{L}\begin{bmatrix} & u_1 & u_2 & v_1 & v_2 \\ & \lambda^2 & & & \\ & -\lambda^2 & \lambda^2 & & \\ & \lambda\mu & -\lambda\mu & \mu^2 & \\ & -\lambda\mu & \lambda\mu & -\mu^2 & \mu^2 \end{bmatrix} \tag{6}$$

As given in Eq. (6), $[K]$ is singular—that is, its determinant vanishes and its inverse does not exist. This is overcome by supplying boundary conditions or supports for the bar sufficient to prevent it from moving as a rigid body. For example, we may choose $u_1 = v_1 = u_2 = 0, v_2 \neq 0$. Node 1 is then fixed, while node 2 is provided with a roller in the y-direction. The only force component now capable of straining the bar is F_{y_2}. The force in the bar and the reactions are given by Eqs. (5) and (6).

Any other physically correct boundary conditions can be imposed. In other words, once $[K]$ has been determined, a solution can be found for any set of support conditions. The only requirement is that the structure be fixed against rigid body displacement.

(VI) Stiffness Analysis of Simple Truss

Once stiffness matrices for the various component units of a structure have been determined, the next step of finding the stiffness of the composite structure may be taken. The procedure for doing this is essentially independent of the complexity of the structure. As a result, it will be illustrated for a simple truss as shown in Fig. 2.

The stiffness of any one member of the truss is given by Eq. (6). Since length varies for the truss members, this term should be brought inside the matrix. It is then convenient to call the elements of the stiffness matrix $\bar{\lambda}^2 = \lambda^2/\text{length}$, etc. Then $\bar{\lambda}^2$, $\bar{\mu}^2$, and $\bar{\lambda}\bar{\mu}$ represent the essential terms defining the stiffness of the separate truss members. These are conveniently calculated by setting up Table 1.

From the last three columns of Table 1 the truss stiffness matrix can be written directly. This is best seen by forming the truss equation [Eq. (7a)] analogous to Eq. (5) for the single member.

The formation of all columns in Eq. (7a) can be explained by considering any one of them as an example. The second column will be chosen. It represents the case for which $v_1 \neq 0$, all other node displacements = 0.

$$\begin{Bmatrix} F_{x_1} \\ F_{y_1} \\ F_{x_2} \\ F_{y_2} \\ F_{x_3} \\ F_{y_3} \end{Bmatrix} = AE \begin{bmatrix} \frac{1}{2\sqrt{2}L} & -\frac{1}{2\sqrt{2}L} & 0 & 0 & -\frac{1}{2\sqrt{2}L} & \frac{1}{2\sqrt{2}L} \\ -\frac{1}{2\sqrt{2}L} & \frac{1}{L}+\frac{1}{2\sqrt{2}L} & 0 & -\frac{1}{L} & \frac{1}{2\sqrt{2}L} & -\frac{1}{2\sqrt{2}L} \\ 0 & 0 & \frac{1}{L} & 0 & -\frac{1}{L} & 0 \\ 0 & -\frac{1}{L} & 0 & \frac{1}{L} & 0 & 0 \\ -\frac{1}{2\sqrt{2}L} & \frac{1}{2\sqrt{2}L} & -\frac{1}{L} & 0 & \frac{1}{L}+\frac{1}{2\sqrt{2}L} & -\frac{1}{2\sqrt{2}L} \\ \frac{1}{2\sqrt{2}L} & -\frac{1}{2\sqrt{2}L} & 0 & 0 & -\frac{1}{2\sqrt{2}L} & \frac{1}{2\sqrt{2}L} \end{bmatrix} \begin{Bmatrix} u_1 \\ v_1 \\ u_2 \\ v_2 \\ u_3 \\ v_3 \end{Bmatrix} \tag{7a}$$

or

$$\{F\} = [K]\{\delta\} \tag{7b}$$

In this second column the y-components of force are given by the $\bar{\mu}^2$ terms in Table 1; the x-components of force are given by the $\bar{\lambda}\bar{\mu}$ terms. Thus F_{y_1} is the sum of $\bar{\mu}^2$ for members 1–2 and 1–3 since these are strained due to displacement v_1. Also F_{y_2} is $-\bar{\mu}^2$ for member 1–2, and F_{y_3} is $-\bar{\mu}^2$ for member 1–3. The signs follow from the basic stiffness matrix given in Eq. (6). Since equilibrium must hold, the sum of these y-components of force must vanish.

Similarly, F_{x_1} is the sum of the $\bar{\lambda}\bar{\mu}$ terms for members 1–2 and 1–3. Likewise, F_{x_2} is the negative value of $\bar{\lambda}\bar{\mu}$ for member 1–2. Finally F_{x_3} is $-\bar{\lambda}\bar{\mu}$ for member 1–3. These forces must also sum to zero if equilibrium is to hold.

Table 1

Member	x	y	Length	λ	μ	λ^2	μ^2	$\lambda\mu$	$\bar{\lambda}^2$	$\bar{\mu}^2$	$\bar{\lambda}\bar{\mu}$
1–2	0	$-L$	L	0	-1	0	1	0	0	$\frac{1}{L}$	0
1–3	L	$-L$	$\sqrt{2}L$	$\frac{1}{\sqrt{2}}$	$-\frac{1}{\sqrt{2}}$	$\frac{1}{2}$	$\frac{1}{2}$	$-\frac{1}{2}$	$\frac{1}{2\sqrt{2}L}$	$\frac{1}{2\sqrt{2}L}$	$-\frac{1}{2\sqrt{2}L}$
2–3	L	0	L	1	0	1	0	0	$\frac{1}{L}$	0	0

This process is repeated for all columns. In this way all possible node displacement components are taken into account. In each case the displacements are compatible ones for all members of the truss.

A structure having various kinds of structural components—beams as well as axially loaded members, for example—would be treated in the same manner. However, the basic stiffness matrix for each type of member would have to be known. Deriving these for units of interest in aircraft design represents a major part of this paper.

The matrix of Eq. (7a) is singular. This is altered by providing supports for the truss sufficient to prevent it from displacing as a rigid body when loads are applied. Any sufficient set of supports may be imposed; here we choose to put

$$u_1 = v_1 = u_2 = v_2 = 0$$

In other words, nodes 1 and 2 are fixed, while 3 is left free.

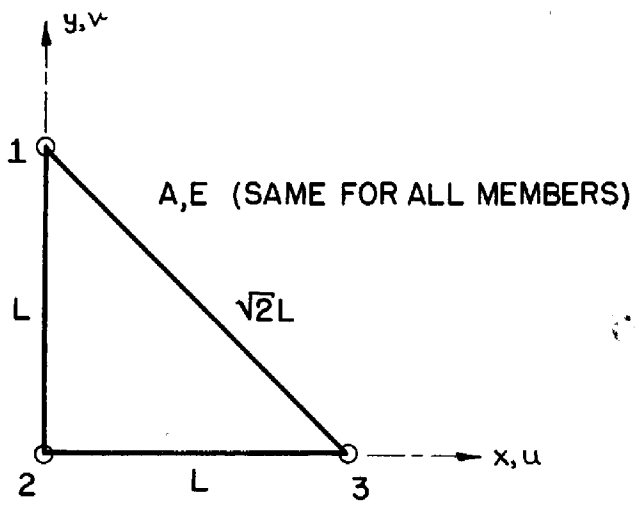

FIG. 2. Simple truss.

It is now convenient to rewrite Eq. (7a) and simultaneously partition it as shown by the broken lines in Eq. (7c).

$$\begin{Bmatrix} F_{x_3} \\ F_{y_3} \\ \hline F_{x_1} \\ F_{y_1} \\ F_{x_2} \\ F_{y_2} \end{Bmatrix} = \frac{AE}{L} \left[\begin{array}{cc|cc|cc} 1+\frac{1}{2\sqrt{2}} & -\frac{1}{2\sqrt{2}} & -\frac{1}{2\sqrt{2}} & \frac{1}{2\sqrt{2}} & -1 & 0 \\ -\frac{1}{2\sqrt{2}} & \frac{1}{2\sqrt{2}} & \frac{1}{2\sqrt{2}} & -\frac{1}{2\sqrt{2}} & 0 & 0 \\ \hline -\frac{1}{2\sqrt{2}} & \frac{1}{2\sqrt{2}} & \frac{1}{2\sqrt{2}} & -\frac{1}{2\sqrt{2}} & 0 & 0 \\ \frac{1}{2\sqrt{2}} & -\frac{1}{2\sqrt{2}} & -\frac{1}{2\sqrt{2}} & 1+\frac{1}{2\sqrt{2}} & 0 & -1 \\ -1 & 0 & 0 & 0 & 1 & 0 \\ 0 & 0 & 0 & -1 & 0 & 1 \end{array}\right] \begin{Bmatrix} u_3 \\ v_3 \\ \hline u_1 = 0 \\ v_1 = 0 \\ u_2 = 0 \\ v_2 = 0 \end{Bmatrix} \tag{7c}$$

If the partitioned square (stiffness) matrix is designated by

$$\left[\begin{array}{c|c} A_{2\times 2} & B_{2\times 4} \\ \hline B'_{4\times 2} & D_{4\times 4} \end{array}\right]$$

expanding Eq. (7c) leads to the following two sets of equations:

$$\begin{Bmatrix} F_{x_3} \\ F_{y_3} \end{Bmatrix} = [A] \begin{Bmatrix} u_3 \\ v_3 \end{Bmatrix} \tag{8a}$$

and

$$\begin{Bmatrix} F_{x_1} \\ F_{y_1} \\ F_{x_2} \\ F_{y_2} \end{Bmatrix} = [B]' \begin{Bmatrix} u_3 \\ v_3 \end{Bmatrix} \tag{8b}$$

Eq. (8a) gives unknown node displacements in terms of applied forces,

$$\begin{Bmatrix} u_3 \\ v_3 \end{Bmatrix} = [A]^{-1} \begin{Bmatrix} F_{x_3} \\ F_{y_3} \end{Bmatrix} \tag{9a}$$

while Eq. (8b), together with Eq. (9a), gives unknown reactions in terms of applied forces,

$$\begin{Bmatrix} F_{x_1} \\ F_{y_1} \\ F_{x_2} \\ F_{y_2} \end{Bmatrix} = [B]' [A]^{-1} \begin{Bmatrix} F_{x_3} \\ F_{y_3} \end{Bmatrix} \tag{9b}$$

In dynamic analyses of aircraft structures it is ordinarily sufficient to determine $[A]^{-1}$. This is the flexibility matrix. It is interesting to note that $[A]$ can be found from the complete $[K]$ matrix by merely striking out columns and rows corresponding to zero displacements as prescribed by the support conditions.

A complete stress analysis leading to the truss member forces can also be carried out. It is merely necessary to know the force-deflection relations for the individual members, or components, of the structure. This is a straightforward problem for the truss and, therefore, will not be discussed further in this paper.

It is worth while to notice that once the stiffness matrix has been written, the solution follows by a series of routine matrix calculations. These are rapidly carried out on automatic digital computing equipment. Changes in design are taken care of by properly modifying the stiffness matrix. This cuts

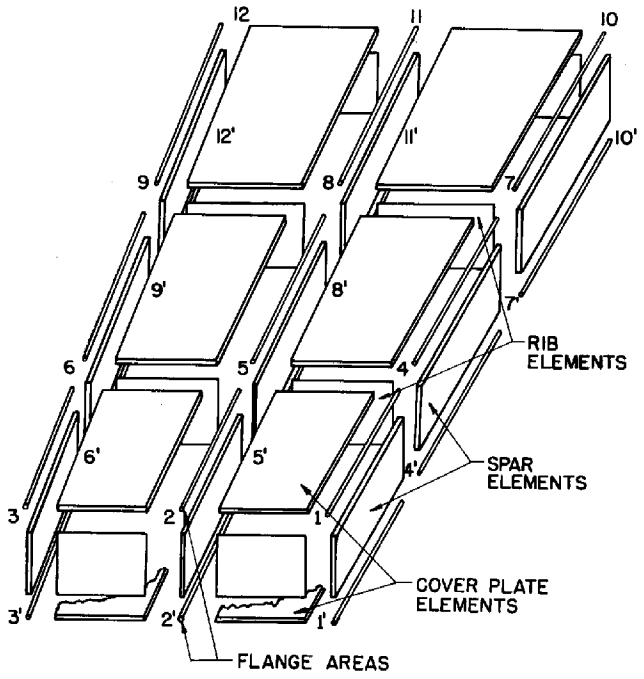

FIG. 3. Wing structure breakdown.

analysis time to a minimum, since development of the stiffness matrix is also a routine procedure. In fact, it may also be programmed for the digital computing machine.

(VII) SUMMARY—METHOD OF DIRECT STIFFNESS CALCULATION

(1) A complex structure must first be replaced by an equivalent idealized structure consisting of basic structural parts that are connected to each other at selected node points.

(2) Stiffness matrices must be either known or determined for each basic structural unit appearing in the idealized structure.

(3) While all other nodes are held fixed, a given node is displaced in one of the chosen coordinate directions. The forces required to do this and the reactions set up at neighboring nodes are then known from the various individual member stiffness matrices. These forces and reactions determine one column in the overall stiffness matrix. When all components of displacement at all nodes have been considered in this manner, the complete stiffness matrix will have been developed. In the general case, this matrix will be of order $3n \times 3n$, where n equals the number of nodes. The stiffness matrix so developed will be singular.

(4) Desired support conditions can be imposed by striking out columns and corresponding rows, in the stiffness matrix, for which zero displacements have been specified. This reduces the order of the stiffness matrix and renders it nonsingular.

(5) For any given set of external forces at the nodes, matrix calculations applied to the stiffness matrix then yield all components of node displacement plus the external reactions.

(6) Forces in the internal members can be found by applying the appropriate force-deflection relations.

The primary functions of the engineer will be to provide the information required in steps (1) and (2) above and to provide the individual member force-deflection relations if a stress analysis is to be carried out. Steps (3) through (6) can be performed by non-engineering trained personnel. Changes in design can be taken into account by correcting local stiffness contributions to K. Node densities can be increased in regions of maximum complexity and importance. If vertical deflections only are required, as in the case of the aircraft wing problem, the $3n \times 3n$ matrix for K can be reduced to order $n \times n$ by a sequence of matrix calculations. Physically, continuity of displacements in three directions at each node will still be maintained.

(VIII) STIFFENED SHELL STRUCTURES

In carrying the above procedure over to stiffened shell structures, it is first necessary to perform steps (1) and (2) of the previous outline.

For a wing structure the idealization will be made by replacing the actual structure by an assemblage of spar segments, rib segments, stiffeners, and cover plate elements, joined together at selected nodes. Fig. 3 shows the proposed idealized structure. The decomposition of the structure can be carried further with some increase in accuracy (for example, by decomposing spar segments into spar caps and shear webs), or it can be simplified by treating the structure as an assemblage of spars and torque boxes. The degree of breakdown should be consistent with the complexity of structural deformations required by the problem at hand. (In a vibration analysis the order of the highest mode is a determining factor.) In light of the proposed idealization, it is necessary that stiffness matrices be developed for the following components: beam segments consisting of flanges joined by thin webs, and plate elements of arbitrary shape. In addition, provision must be made for taking stiffeners into account and possibly for including the effect of sandwich type skin panels.

In the general case, spars will be swept, nonparallel, and not necessarily orthogonal to ribs. It will generally be convenient to transfer stiffness values for any given member to a fixed set of reference axes. These reference axes will be chosen as rectangular Cartesian (x, y, z) in order to preserve symmetry in the total K-matrix.

An outline of the determination of member stiffness for simple structural elements is given in the paper. Further details are presented in Appendixes. Derivation of stiffness matrices for more complex elements can be accomplished in a straightforward manner. However, in the analysis of an actual structure, it will be necessary to weigh the relative advantages of employing a small number of large complex elements against the advantages of using a larger number of small elements for which simple stiffness coefficients

may be employed. The main criterion to be observed in resolving this issue is that the problem must be programmed so that as much as possible of the data processing is performed automatically by the computer and not by human operators substituting in complex formulas.

(IX) Spars and Ribs

First we consider the untapered beam segment of uniform cross section shown in Fig. 4. Its stiffness matrix will be determined by application of beam theory, which is extended, however, to include shear web flexibility.

Nodes, 1, 1′, 2, and 2′ are established as shown in Fig. 4. The following notation is used:

I = moment of inertia of beam section about neutral (y) axis
$t_w = t$ = thickness of shear web
E = modulus of elasticity of flange material
G = modulus of rigidity of shear web material
ν = Poisson ratio

Displacements are assumed such as to be compatible with elementary beam theory. In other words,

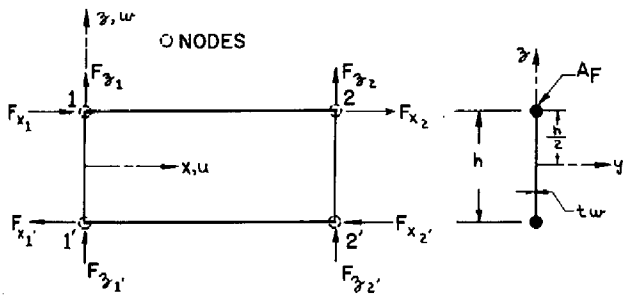

Fig. 4. Beam (spar or rib) segment.

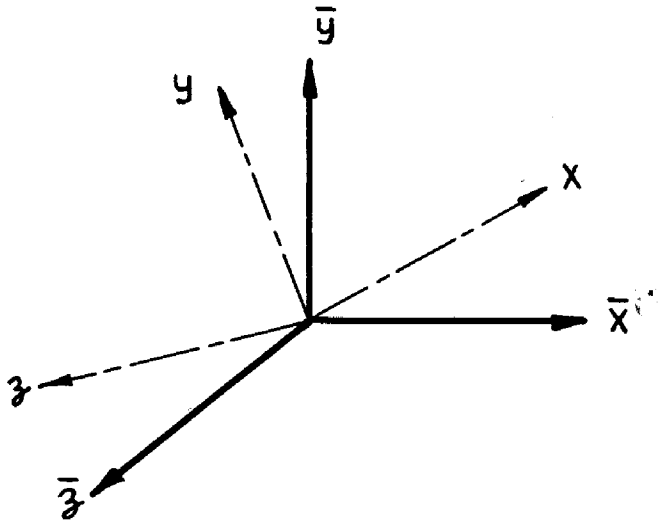

Fig. 5. Rectangular Cartesian axes systems.

$$\left.\begin{aligned} w_1 &= w_{1'}, & w_2 &= w_{2'} \\ u_1 &= -u_{1'}, & u_2 &= -u_{2'} \end{aligned}\right\} \tag{10}$$

Stiffness in the y-direction is assumed negligible.

An outline of the derivation of the stiffness matrix for the above beam segment is given in Appendix (A). It is shown to be of the form

$$[K] = \frac{6EI}{Lh^2(1+4n)} \begin{bmatrix} u_1 & v_1 & w_1 & u_2 & v_2 & w_2 \\ (4/3)\ (1+n) & & & & & \\ 0 & 0 & & & & \\ -(h/L) & 0 & h^2/L^2 & & & \\ (2/3)\ (1-2n) & 0 & -(h/L) & (4/3)\ (1+n) & & \\ 0 & 0 & 0 & 0 & 0 & \\ h/L & 0 & -(h^2/L^2) & h/L & 0 & h^2/L^2 \end{bmatrix} \tag{11a}$$

where $$n = 3(E/G)\ [I/(htL^2)] \tag{11b}$$

Contribution of shear web deformation to the above stiffness matrix is indicated by values of $n > 0$; for a rigid shear web $n = 0$.

As a simple example of the use of the beam stiffness matrix, we consider a cantilever of length L and loaded by force P at the free end (nodes 1 and 1′). Putting $n = 0$ and applying Eq. (11a) gives:

$$\begin{Bmatrix} F_{x_2} \\ F_{z_2} \end{Bmatrix} = \frac{6EI}{L^3} \begin{bmatrix} \frac{4}{3}\frac{L^2}{h^2} & \frac{L}{h} \\ \frac{L}{h} & 1 \end{bmatrix} \begin{Bmatrix} u_2 \\ w_2 \end{Bmatrix} \tag{12}$$

Eq. (12) may be inverted to yield tip displacements u_1 and w_1 in terms of applied load P ($F_{x_1} = 0$, $F_{z_1} = P/2$). The results are

$$u_2 = -(PL^2/2EI)\ (h/2), \qquad w_2 = PL^3/3EI$$

which agree with known results.

In an actual wing structure, spar and rib segments will be more or less randomly oriented with respect to a set of standard reference axes. As a result, transformation of stiffness matrices for these members to the standard set of axes will generally be necessary. The basis for such transformations is given below.

Let the direction cosines of x, y, z-axes with respect to standard $\bar{x}$, $\bar{y}$, $\bar{z}$-axes, Fig. 5, be

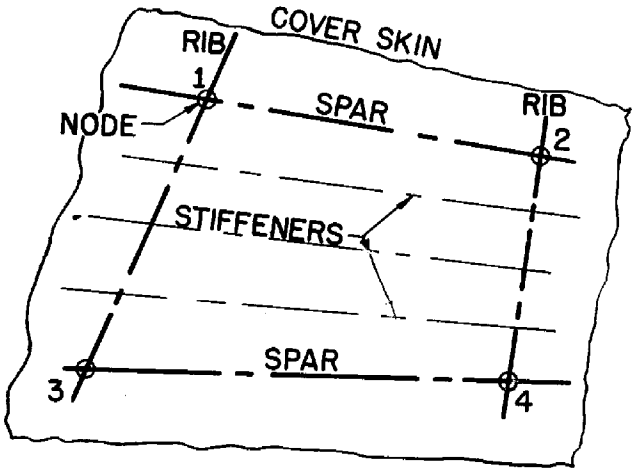

FIG. 6. Stiffened cover skin element.

	x	y	z
$\bar{x}$	λ_x	λ_y	λ_z
$\bar{y}$	μ_x	μ_y	μ_z
$\bar{z}$	ν_x	ν_y	ν_z

Simple geometrical considerations then give the following equation for relating forces in the x, y, z system to forces in the $\bar{x}$, $\bar{y}$, $\bar{z}$ system:

$$\begin{Bmatrix} F_{\bar{x}_1} \\ F_{\bar{y}_1} \\ F_{\bar{z}_1} \\ F_{\bar{x}_2} \\ F_{\bar{y}_2} \\ F_{\bar{z}_2} \end{Bmatrix} = \begin{bmatrix} \lambda_x & \lambda_y & \lambda_z & 0 & 0 & 0 \\ \mu_x & \mu_y & \mu_z & 0 & 0 & 0 \\ \nu_x & \nu_y & \nu_z & 0 & 0 & 0 \\ 0 & 0 & 0 & \lambda_x & \lambda_y & \lambda_z \\ 0 & 0 & 0 & \mu_x & \mu_y & \mu_z \\ 0 & 0 & 0 & \nu_x & \nu_y & \nu_z \end{bmatrix} \cdot \begin{Bmatrix} F_{x_1} \\ F_{y_1} \\ F_{z_1} \\ F_{x_2} \\ F_{y_2} \\ F_{z_2} \end{Bmatrix} \tag{13a}$$

or,

$$\{\bar{F}\} = [\Phi]\{F\} \tag{13b}$$

Displacements are vectors similarly related to the coordinate systems as forces and hence transform under a rotation of axes in the same manner. Consequently,

$$\{\bar{\delta}\} = [\Phi]\{\delta\} \tag{14}$$

where

$$\{\bar{\delta}\} = \begin{Bmatrix} \bar{u}_1 \\ \bar{v}_1 \\ \cdot \\ \cdot \\ \cdot \\ \bar{w}_2 \end{Bmatrix} \text{ etc.}$$

From the above and Eq. (3) it follows that,

$$[\bar{K}] = [\Phi][K][\Phi]^{-1} = [\Phi][K][\Phi]' \tag{15}$$

where $[\bar{K}]$ is the stiffness matrix referred to the standard $\bar{x}$, $\bar{y}$, $\bar{z}$ set of axes. Beam segments encountered in the analysis of real structures will be tapered in depth, and flange areas will be variable; generally the segments will be taken short enough so that the variation in depth may be assumed linear. Derivation of stiffness matrices for elements of this kind is straightforward, and details will not be included in the present paper.

(X) Stiffened Plates

(1) *Stiffeners*

A plan view of a typical portion of stiffened cover skin structure is shown in Fig. 6. Nodes are initially established at points 1, 2, 3, and 4. The included structure then consists of spar segments (1–2 and 3–4), rib segments (1–3 and 2–4), and stiffened plate element 1–2–3–4. Stiffeners may be conveniently lumped with spar caps and, if desired, into one or more equivalent stiffeners located between spars. In this latter event additional nodes must be established, as at the intersections of these equivalent stiffeners with the ribs. The stiffness matrix for a lumped stiffener of constant area A, length L, and modulus E is

$$[K]_{\text{stiffener}} = \frac{AE}{L}\begin{bmatrix} 1 & -1 \\ -1 & 1 \end{bmatrix} \tag{16}$$

Derivation of a similar matrix for a tapered member is straightforward; the area A is replaced by a suitable mean value. The influence of shear lag effects on load-deflection relations for the panel and stiffeners can only be included if nodes are established at intermediate points on the ribs, between spars.

(2) *Plate Stiffness*

The quadrilateral plate element 1–2–3–4 of Fig. 6 is assumed to possess in-plane stiffness only. Since two independent displacement components can occur at each node, the order of the K-matrix for this plate element will be 8×8. The problem of calculating K is not an easy one, and the solution offered here is felt to have potential usefulness for finding approximate solutions to many two-dimensional problems in elasticity.

Before proceeding with the method developed for calculating K of the plate element, it is pointed out that a so-called framework analogy[12] exists, which permits one to replace the elastic plate with a lattice of elastic bars. Under certain conditions the framework then deforms as does the plate and hence can be used to calculate the plate stiffness. The determination of a lattice representation for a rectangular plate is relatively straightforward; however, plate elements of nonrectangular form present basic difficulties. For example, if one attempts to apply the rectangular gridwork to a nonrectangular plate, difficulties arise in attempting to satisfy boundary conditions. On the other hand, if one goes to nonrectangular lattice forms, difficulties arise when attempting to satisfy the stress-strain relations in the interior of the plate. Considerations such as these led to eventual abandonment of this approach.

The concept finally employed for determining plate stiffness is based on approximating actual plate strains by a restricted strain representation. In other words, no matter what the actual strains in the plate may be, these will be approximated by a superposition of several simple strain states. The method for doing

this and the accuracy of results based on such a representation form an important portion of this paper.

To give an initial illustration, the actual strain distribution in a rectangular plate element can be approximated by superimposing the strains that correspond to each of the simple external load states shown in Fig. 7. These load states are seen to represent uniform and linearly varying stresses plus constant shear, along the plate edges. Later it will be seen that the number of load states must be $2n - 3$, where n = number of nodes.

Before commenting further on the scheme suggested here for analyzing plate elements, the method will be applied to the triangular plate of Fig. 8. The triangle is not only simpler to handle than the rectangle but later it will be used as the basic "building block" for calculating stiffness matrices for plates of arbitrary shape.

We start by assuming constant strains, or

$$\left.\begin{aligned} \epsilon_x &= a = (1/E)\,(\sigma_x - \nu\sigma_y) = \partial u/\partial x \\ \epsilon_y &= b = (1/E)\,(\sigma_y - \nu\sigma_x) = \partial v/\partial y \\ \gamma_{xy} &= c = (1/G)\tau_{xy} = (\partial u/\partial y) + (\partial v/\partial x) \end{aligned}\right\} \quad (17a)$$

Later it will be pointed out why we are restricted in the choice of strain expressions. Integrating we find the displacements to be

$$\left.\begin{aligned} u &= ax + Ay + B \\ v &= by + (c - A)x + C \end{aligned}\right\} \quad (17b)$$

where, A, B, and C are constants of integration which define rigid body translation and rotation of the triangle. Hence the triangle can displace as a rigid body in its own plane and undergo uniform straining according to Eq. (17a).

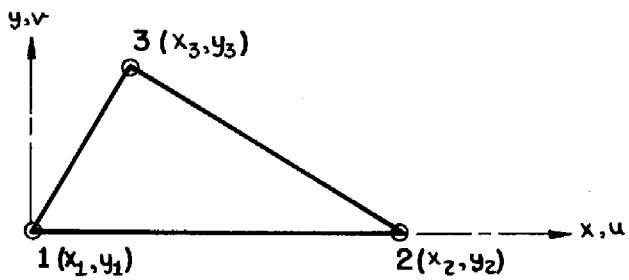

FIG. 8. Node designation for triangular plate element.

Displacements at the nodes can be determined by inserting applicable node coordinates into Eq. (17b). In this way six equations occur which are just sufficient for uniquely determining the six constants of Eq. (17b). As a result the constants become known in terms of node displacements and coordinates. It is this part of the solution which determines the number of terms which must be chosen in the strain expressions or alternatively the number of applied edge stress states which must be used. The number is always twice the number of nodes minus three. Hence, for the triangle we require three terms and five for the rectangle (or quadrilateral).

To proceed with the solution, we solve directly for stresses in terms of node displacements u_1, v_1, u_2, etc. If $x_{ij} = x_i - x_j$ and $\lambda_1 = (1 - \nu)/2$, this gives

$$\begin{Bmatrix} \sigma_x \\ \sigma_y \\ \tau_{xy} \end{Bmatrix} = \frac{E}{1-\nu^2} \begin{bmatrix} -\frac{1}{x_2} & \frac{\nu x_{32}}{x_2 y_3} & \frac{1}{x_2} & -\frac{\nu x_3}{x_2 y_3} & 0 & \frac{\nu}{y_3} \\ -\frac{\nu}{x_2} & \frac{x_{32}}{x_2 y_3} & \frac{\nu}{x_2} & -\frac{x_3}{x_2 y_3} & 0 & \frac{1}{y_3} \\ \frac{\lambda_1 x_{32}}{x_2 y_3} & -\frac{\lambda_1}{x_2} & -\frac{\lambda_1 x_3}{x_2 y_3} & \frac{\lambda_1}{x_2} & \frac{\lambda_1}{y_3} & 0 \end{bmatrix} \begin{Bmatrix} u_1 \\ v_1 \\ u_2 \\ v_2 \\ u_3 \\ v_3 \end{Bmatrix} \quad (18a)$$

or

$$\{\sigma\} = [S]\,\{\delta\} \quad (18b)$$

The next step is to obtain the concentrated forces at the nodes which are statically equivalent to the applied constant edge stresses. The procedure for doing this will be briefly illustrated for the case of the shear stress.

Fig. 9(a) shows the shear stresses on the circumscribed rectangular element, and Fig. 9(b) shows the corresponding edge shear forces on the triangle. As before x_i, y_i refer to coordinates of node points.

Forces on any edge are equally distributed between nodes lying on that edge. For the forces as given in Fig. 9(b), this leads to

$$\left.\begin{aligned} F_{x_1}^{(3)} &= -(x_2 - x_3)\,(t/2)\,\tau_{xy} \\ F_{y_1}^{(3)} &= -y_3(t/2)\,\tau_{xy} \\ F_{x_2}^{(3)} &= -x_3(t/2)\,\tau_{xy} \\ F_{y_2}^{(3)} &= +y_3(t/2)\,\tau_{xy} \\ F_{x_3}^{(3)} &= +x_2(t/2)\,\tau_{xy} \\ F_{y_3}^{(3)} &= 0 \end{aligned}\right\} \quad (19)$$

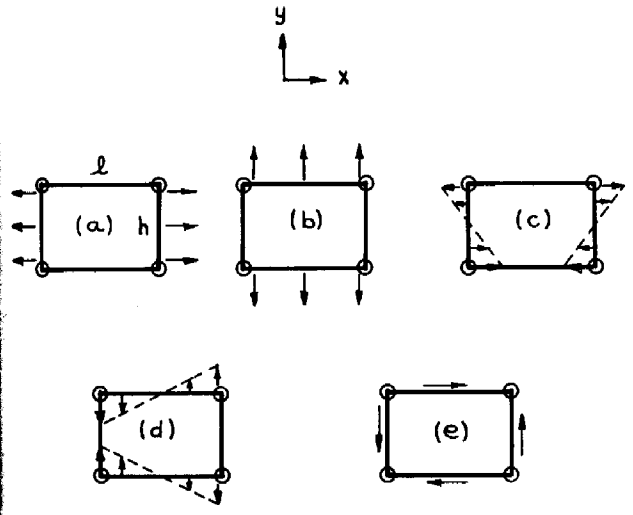

FIG. 7. Applied loads on edges of rectangular plate element.

where the superscript refers to case 3 (that of shear stress). This procedure is repeated for the two normal stresses. Superimposing results for these three cases then leads to the following system of equations for node forces in terms of applied edge stresses:

$$\begin{Bmatrix} F_{x_1} \\ F_{y_1} \\ F_{x_2} \\ F_{y_2} \\ F_{x_3} \\ F_{y_3} \end{Bmatrix} = \frac{t}{2} \begin{bmatrix} -y_3 & 0 & -(x_2 - x_3) \\ 0 & -(x_2 - x_3) & -y_3 \\ y_3 & 0 & -x_3 \\ 0 & -x_3 & y_3 \\ 0 & 0 & x_2 \\ 0 & x_2 & 0 \end{bmatrix} \begin{Bmatrix} \sigma_x \\ \sigma_y \\ \tau_{xy} \end{Bmatrix} \tag{20a}$$

or

$$\{F\} = [T]\{\sigma\} \tag{20b}$$

Substituting Eq. (18b) into Eq. (20b),

$$\{F\} = [T][S]\{\delta\} \tag{20c}$$

Comparing this last equation with Eq. (3) shows that

$$[K] = [T][S] \tag{21}$$

Carrying out the indicated matrix multiplication and putting $\lambda_2 = (1 + \nu)/2$ gives

$$[K]_{\substack{\text{Plate} \\ \text{(triangle)}}} = \frac{Et}{2(1-\nu^2)} \begin{bmatrix} \frac{y_3}{x_2} + \frac{\lambda_1 x_{23}^2}{x_2 y_3} & & & & & \\ -\frac{\lambda_2 x_{32}}{x_2} & \frac{x_{23}^2}{x_2 y_3} + \frac{\lambda_1 y_3}{x_2} & & & & \\ -\frac{y_3}{x_2} + \frac{\lambda_1 x_3 x_{23}}{x_2 y_3} & \frac{\nu x_{32}}{x_2} + \frac{\lambda_1 x_3}{x_2} & \frac{y_3}{x_2} + \frac{\lambda_1 x_3^2}{x_2 y_3} & & & \\ \frac{\nu x_3}{x_2} + \frac{\lambda_1 x_{32}}{x_2} & \frac{x_3 x_{23}}{x_2 y_3} - \frac{\lambda_1 y_3}{x_2} & -\frac{\lambda_2 x_3}{x_2} & \frac{x_3^2}{x_2 y_3} + \frac{\lambda_1 y_3}{x_2} & & \\ -\frac{\lambda_1 x_{23}}{y_3} & -\lambda_1 & -\frac{\lambda_1 x_3}{y_3} & \lambda_1 & \frac{\lambda_1 x_2}{y_3} & \\ -\nu & -\frac{x_{23}}{y_3} & \nu & -\frac{x_3}{y_3} & 0 & \frac{x_2}{y_3} \end{bmatrix} \tag{22}$$

An alternative approach to the above method for calculating the plate stiffness matrix is to calculate the strain energy in the plate due to the assumed strain distribution and to then apply Castigliano's Theorem for finding the node forces. This procedure can also be conveniently carried out in terms of matrix operations; details will not be included here, however, since the result is the same as that already obtained.

Stiffness matrices for plates having four and more nodes have been derived and studied. The advantage in introducing additional nodes lies in the fact that a more general strain expression may then be employed—or equivalently additional load states as illustrated by Fig. 7 may be used for the plate. As a result a choice between two points of view may be adopted; first, the simplest or triangular plate stiffness matrix may be used and the desired accuracy obtained by using a sufficient number of subelements, or second, a more general plate stiffness matrix may be used with fewer subelements. Experience to date indicates that satisfactory results can be obtained using the triangular plate stiffness matrix.

Some additional plate stiffness matrices are given in Appendix (B).

To summarize briefly the meaning and significance of the plate stiffness matrix, it is first pointed out that this matrix relates node forces to node displacements. As a result the plate stiffness can be immediately added to spar, rib, etc., stiffnesses which are also given for specified nodal points. However, the plate node forces are statically equivalent to certain plate edge stresses. Furthermore, these edge stresses will tend to approach actual edge stresses, even of a complex nature, if sufficient subelements are used. A result of these equivalent edge stresses is that continuity will tend to be approximately maintained along common edges of subelements, between nodes. In other words, we are assuming that a plate under complex strains will deform in a manner that can be approximated by relatively simple strains acting on subelements into which the larger plate has been divided. The accuracy of this representation should increase as the number of subelements increases.

(3) *Quadrilateral Plates*

In the analysis of wings and tail surfaces it is generally convenient to employ a subdivision of cover plates such that most elements are of quadrilateral shape. The stiffness matrix for such elements can then be derived in one of two ways: (a) the previous solution demonstrated for the triangle can be extended to include the quadrilateral and (b) the quadrilateral can be subdivided into triangles and its stiffness matrix determined by superposition of the stiffnesses of the individual triangles. In this section the latter procedure will be adopted.

Two simple subdivisions of the quadrilateral into triangles are shown in Figs. 10(a) and 10(*b*). These lead to different stiffness matrices for the quadrilateral. A unique result is obtained by using the subelements shown in Fig. 10(c). The interior node will be located at the centroid, although any other choice could be used.

For the general quadrilateral plate it has proved to be preferable to program the calculation of the stiffness matrix for high-speed computing equipment. In the case of the rectangle, however, an explicit derivation can be readily carried out. The necessary calculations, included below, are given here, since the end result is useful and since these calculations serve to illustrate a step of some importance in carrying out the analysis of a more complete structure—for example, a wing or tail surface.

The rectangle and its four triangular subelements, with interior node number 5 at the centroid, is shown in Fig. 11. Stiffness matrices for the triangles can be calculated from Eq. (22), or more conveniently from Eq. (B-3) of Appendix (B). In determining K of the rectangle, superposition in the following form is used:

$$K_{\text{rectangle}} = K_{\text{I}} + K_{\text{II}} + K_{\text{III}} + K_{\text{IV}}$$

Since five nodes have been established, K for the rectangle will initially be of order 10×10. This will later be reduced to order 8×8 to give a result consistent with the choice of four external nodes; only at these external nodes is contact implied with adjoining structure. The immediate point is, however, that K for each triangle must be increased to order 10×10 before superposition is carried out. This is accomplished in the usual way—that is, by introducing appropriate rows and columns of zero elements.

In order to simplify the expressions for elements appearing in the stiffness matrices the derivation of K for the rectangle will be restricted to $\nu = 1/3$.

On superimposing stiffnesses for the component triangles of Fig. 11 it becomes possible to express Eq. (3) in the form

$$\begin{Bmatrix} F_{x_1} \\ F_{x_2} \\ F_{x_3} \\ F_{x_4} \\ F_{y_1} \\ F_{y_2} \\ F_{y_3} \\ F_{y_4} \\ \hline F_{x_5} \\ F_{y_5} \end{Bmatrix} = \left[\begin{array}{c|c} A_{8\times 8} & B_{8\times 2} \\ \hline B'_{2\times 8} & C_{2\times 2} \end{array}\right] \begin{Bmatrix} u_1 \\ u_2 \\ u_3 \\ u_4 \\ v_1 \\ v_2 \\ v_3 \\ v_4 \\ \hline u_5 \\ v_5 \end{Bmatrix} \tag{23}$$

Since forces are to be applied to the rectangle by stresses equivalent to forces acting at nodes 1, 2, 3, and 4, the condition

$$F_{x_5} = F_{y_5} = 0$$

can be applied to Eq. (23). Doing this results in the two sets of equations written below:

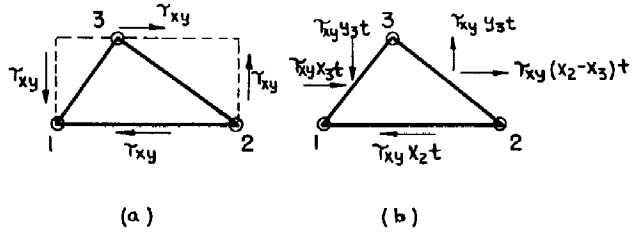

FIG. 9. Shear loading on triangular plate element.

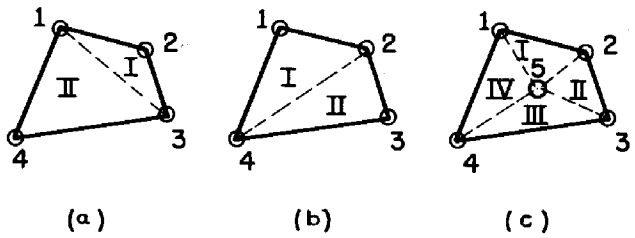

FIG. 10. Decomposition of quadrilateral plate into triangular subelements.

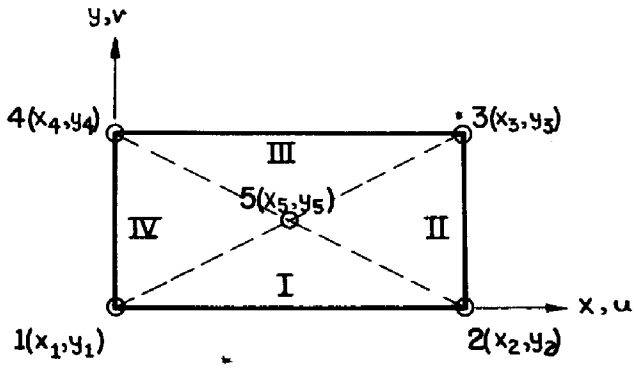

FIG. 11. Triangular subelements for rectangular plate.

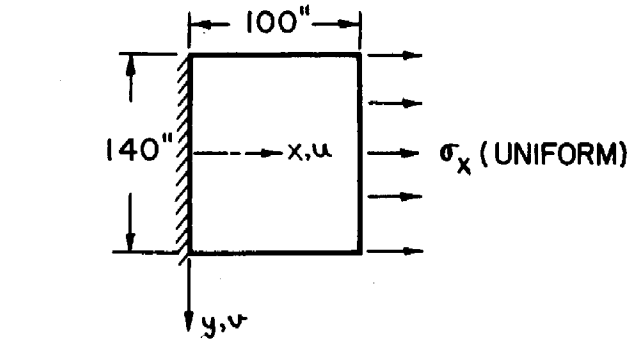

FIG. 12. Clamped rectangular plate subjected to uniform tensile loading.

$$\begin{Bmatrix} F_{x_1} \\ F_{x_2} \\ F_{x_3} \\ F_{x_4} \\ F_{y_1} \\ F_{y_2} \\ F_{y_3} \\ F_{y_4} \end{Bmatrix} = [A] \begin{Bmatrix} u_1 \\ u_2 \\ u_3 \\ u_4 \\ v_1 \\ v_2 \\ v_3 \\ v_4 \end{Bmatrix} + [B] \begin{Bmatrix} u_5 \\ v_5 \end{Bmatrix} \tag{24a}$$

$$\begin{Bmatrix} 0 \\ 0 \end{Bmatrix} = [B]' \begin{Bmatrix} u_1 \\ u_2 \\ u_3 \\ u_4 \\ v_1 \\ v_2 \\ v_3 \\ v_4 \end{Bmatrix} + [C] \begin{Bmatrix} u_5 \\ v_5 \end{Bmatrix} \tag{24b}$$

Solving Eq. (24b) for displacements at node 5 and substituting the result into Eq. (24a),

$$\begin{Bmatrix} F_{xi} \\ F_{yi} \end{Bmatrix} = ([A] - [B]\,[C]^{-1}\,[B]') \begin{Bmatrix} u_i \\ v_i \end{Bmatrix} \tag{25}$$

where $i = 1, 2, 3, 4$. Comparing Eq. (25) with Eq. (3) gives

$$[K]_{\text{rectangle}} = [A] - [B]\,[C]^{-1}\,[B]' \tag{26}$$

Carrying out the calculations required by Eq. (26) results in the following rectangular plate stiffness matrix:

$$[K]_{\text{rectangle}} = \frac{3Et}{16} \left[\begin{array}{c|c} K_{11} & K_{12} \\ \hline K_{21} & K_{22} \end{array}\right] \tag{27a}$$

where, when $m = (x_2 - x_1)/(y_4 - y_1)$,

$$K_{11} = \frac{1}{4} \begin{array}{c} \begin{matrix} u_1 & \quad u_2 & \quad u_3 & \quad u_4 \end{matrix} \\ \begin{bmatrix} 3m + \frac{9}{m} & & & \\ m - \frac{9}{m} & 3m + \frac{9}{m} & & \\ -m - \frac{3}{m} & -3m + \frac{3}{m} & 3m + \frac{9}{m} & \\ -3m + \frac{3}{m} & -m - \frac{3}{m} & m - \frac{9}{m} & 3m + \frac{9}{m} \end{bmatrix} \end{array} + \frac{1}{3m + \frac{1}{m}} \begin{array}{c} \begin{matrix} u_1 & u_2 & u_3 & u_4 \end{matrix} \\ \begin{bmatrix} -1 & & & \\ 1 & -1 & & \\ -1 & 1 & -1 & \\ 1 & -1 & 1 & -1 \end{bmatrix} \end{array} \tag{27b}$$

$$K_{22} = \frac{1}{4} \begin{array}{c} \begin{matrix} v_1 & \quad v_2 & \quad v_3 & \quad v_4 \end{matrix} \\ \begin{bmatrix} 9m + \frac{3}{m} & & & \\ 3m - \frac{3}{m} & 9m + \frac{3}{m} & & \\ -3m - \frac{1}{m} & -9m + \frac{1}{m} & 9m + \frac{3}{m} & \\ -9m + \frac{1}{m} & -3m - \frac{1}{m} & 3m - \frac{3}{m} & 9m + \frac{3}{m} \end{bmatrix} \end{array} + \frac{1}{m + \frac{3}{m}} \begin{array}{c} \begin{matrix} v_1 & v_2 & v_3 & v_4 \end{matrix} \\ \begin{bmatrix} -1 & & & \\ 1 & -1 & & \\ -1 & 1 & +1 & \\ 1 & -1 & 1 & -1 \end{bmatrix} \end{array} \tag{27c}$$

$$K_{12} = \begin{array}{c} \begin{matrix} v_1 & v_2 & v_3 & v_4 \end{matrix} \\ \begin{bmatrix} 1 & & & \\ 0 & -1 & & \\ -1 & 0 & 1 & \\ 0 & 1 & 0 & -1 \end{bmatrix} \end{array} \tag{27d}$$

$$K_{21} = K_{12}' \tag{27e}$$

If the order of v-terms in the above equations are rearranged from v_1, v_2, v_3, v_4 to v_1, v_4, v_3, v_2, it will be discovered that K_{22} equals K_{11} provided we replace m in K_{11} everywhere by $1/m$. The corresponding form for K_{12} may be written without difficulty. It is again pointed out that the above plate stiffness matrix is based on $\nu = 1/3$.

The process of eliminating displacements at node 5 is similar to the situation that arises when only w displacements are to be retained in a wing analysis. In this latter problem it then becomes necessary to eliminate all u and v components of displacement. The procedure for doing this is the same as that used in eliminating u_5 and v_5 from the above problem of the rectangular plate.

(4) *Example*

It is of interest to carry out calculations on a simple example and compare results obtained by applying the plate stiffness matrix with values that can be regarded as correct.

For this purpose the plate of Fig. 12 is analyzed using several different methods. Deflections at several points due to the indicated loading will be calculated. Since an exact solution is not available, correct displacements

TABLE 2

Solution No.	Method	Fig.	u_1	u_2	u_3	u_4	u_5	v_1	v_3	v_4
			Multiply all values by 10^{-6}							
1	Relaxation	13	2.703	2.607	2.703	1.391	1.248	0.686	−0.685	0.562
2	Simple theory	13	2.721	2.721	2.721	1.360	1.360	0.635	−0.635	
3	Plate K-matrix	13a	2.595		2.595			0.740	−0.740	
4	Plate K-matrix	13b	2.692	2.578	2.692	1.355	1.199	0.680	−0.680	0.568
5	Plate K-matrix	13c	2.718		2.697			0.686	−0.717	
6	Plate K-matrix	13d	2.714		2.712			0.688	−0.691	

will be taken as those calculated by applying the relaxation method to the fundamental equations governing this problem. Although details of these calculations are not presented, results are listed in Table 2.

The problem is interesting for at least two reasons. First, the accuracy obtainable using various numbers of subelements can be observed, and second, the effect of using random orientation of subelements—with respect to the plate edges—can be observed.

Results of all calculations are summarized in Table 2. Node locations and subelements are illustrated in Fig. 13.

In Table 2 the solution based on simple theory was obtained from $u = PL/AE$ and $\epsilon_y = -\nu\,\epsilon_x$. It is observed that on this basis both u_1 and v_1 agree quite well with the relaxation solution.

The crudest plate matrix solution is listed in Table 2 as Solution No. 3. It was obtained by considering the plate as a single element whose stiffness is given by Eq. (27). The results for u_1 and v_1 are seen to be reasonably good. Solution No. 4 considers the plate as consisting of four rectangular subelements as shown in Fig. 13(b). Again the stiffness matrix was obtained by using Eq. (27), this time for each subelement. Agreement with relaxation results is seen to be satisfactory, particularly in regard to u_1. Also the differences between u_1 and u_2 are approximated accurately by this solution. It is to be remembered that the actual strain distribution in the plate is complex in nature.

Solutions 5 and 6 in Table 2 were carried out in a matter of minutes on a high-speed digital computer. Each subquadrilateral was considered as consisting of four triangles in a manner analogous to the treatment described previously for the rectangle of Fig. 11. In Solution No. 5 we note that u_1 and u_3 are not equal, a consequence of the random nature of orientation of the subelements. By increasing the number of random subelements as in Solution No. 6, this lack of symmetry in results is virtually removed. Comparison with relaxation values is seen to be very good for both Solutions 5 and 6.

A more comprehensive example is given in the next section of the paper.

(XI) Analysis of Box Beam

As a final example, the box beam of Fig. 14 will be analyzed for deflections, using the stiffness matrices previously derived.

The box is uniform in section, unswept, and contains a rib at the unsupported end. The following dimensions apply: $a/b = \pi$, $2b/h = 10$, $t_c = t_w = t = 0.05$ in., $A_F = bt/2$, $a = 400$ in.

As the simplest possible breakdown, we consider the box to consist of two spars, one rib, and two cover skins. The nodes are then as shown in Fig. 15. Forces may be applied at the nodes at the free end. Two cases will be investigated: (1) up loads at each spar (bending) and (2) up load on one spar and a down load at the other spar (twisting).

The spar matrix is given by Eq. (11a). Calculation shows it to be

$$[K]_{\text{spar}} = \frac{Et}{2}\begin{array}{c} \\ \\ \\ \\ \end{array}\begin{array}{c} \begin{array}{cccc} u_1 \text{ or } u_2 & w_1 \text{ or } w_2 & u_3 \text{ or } u_4 & w_3 \text{ or } w_4 \end{array} \\ \begin{bmatrix} 1.13903 & & & \\ 0.05227 & 0.00333 & & \\ 0.50303 & 0.05227 & 1.13903 & \\ -0.05227 & -0.00333 & -0.05227 & 0.00333 \end{bmatrix} \end{array} \tag{28}$$

Cover plate stiffness is given by Eq. (27a) and for this case becomes

$$[K]_{\text{cover plate}} = \frac{Et}{2}\begin{array}{c} \begin{array}{cccccccc} u_1 & v_1 & u_2 & v_2 & u_3 & v_3 & u_4 & v_4 \end{array} \\ \begin{bmatrix} 0.90878 & & & & & & & \\ -0.37500 & 1.39778 & & & & & & \\ -0.19329 & 0 & 0.90879 & & & & & \\ 0 & -1.15928 & 0.37500 & 1.39778 & & & & \\ -0.31916 & 0 & -0.39634 & -0.37500 & 0.90879 & & & \\ 0 & 0.37109 & -0.37500 & -0.60959 & 0.37500 & 1.39778 & & \\ -0.39634 & 0.37500 & -0.31916 & 0 & -0.19329 & 0 & 0.90879 & \\ 0.37500 & -0.60959 & 0 & 0.37109 & 0 & -1.15928 & -0.37500 & 1.39778 \end{bmatrix} \end{array} \tag{29}$$

The rib has not been defined as yet. Two possible rib configurations will be analyzed in this paper. In the first case, the rib is considered as a beam identical in section to the spar. This leads to the following stiffness matrix for the rib:

$$[K]_{\text{rib}} = \frac{Et}{2}\begin{array}{c} \begin{matrix} v_1 & w_1 & v_2 & w_2 \end{matrix} \\ \begin{bmatrix} 0.13086 & & & \\ -0.00976 & 0.00098 & & \\ 0.06413 & -0.00976 & 0.13086 & \\ 0.00976 & -0.00098 & 0.00976 & 0.00098 \end{bmatrix} \end{array} \tag{30a}$$

In the second case, the rib is treated as a flat plate. The general stiffness matrix which has been derived for a rectangular flat plate is of order 8×8. However, in the present instance, the following conditions must be introduced to insure compatibility with the other portions of the structure (see Fig. 15 for subscript locations):

$$w_1 = w_{1'} \qquad v_1 = -v_{1'}$$
$$\text{and}$$
$$w_2 = w_{2'} \qquad v_2 = -v_{2'}$$

and, likewise, for the forces

$$F_{z_1} = F_{z_{1'}} \qquad F_{y_1} = -F_{y_{1'}}$$
$$\text{and}$$
$$F_{z_2} = F_{z_{2'}} \qquad F_{y_2} = -F_{y_{2'}}$$

Treating the rib as a flat plate ($t = 0.050$ in.) and applying the above conditions leads to the following rib stiffness matrix:

$$[K]_{\text{rib}} = \frac{Et}{2}\begin{array}{c} \begin{matrix} v_1 & w_1 & v_2 & w_2 \end{matrix} \\ \begin{bmatrix} 5.65088 & & & \\ -0.37500 & 0.03754 & & \\ 1.84181 & -0.37500 & 5.65088 & \\ 0.37500 & -0.03754 & 0.37500 & 0.03754 \end{bmatrix} \end{array} \tag{30b}$$

It is anticipated that the choice of rib will have little effect on deflections due to the bending-type loading and a more pronounced effect on the twisting-type loading.

Using the same technique as described for the simple truss, it is now a straightforward matter to form the stiffness matrix for the complete box. Advantage can be taken of the following: (1) structural symmetry that exists for the box with respect to the xy-midplane and (2) restriction in this problem to loads that act normal to this plane. Under these conditions each pair of upper and lower surface nodes will experience, in addition to equal vertical deflections, equal but opposite displacements with respect to the xy-midplane. In other words, the box will deflect in the sense of a conventional beam. The spar and rib stiffness matrices already provide for such elastic behavior. The plate stiffness matrices make no distinction, other than in the sign of the node forces, for a reversal in direction of node displacement. Consequently, if the normal loading is carried equally by upper and lower nodes, only the upper set will need be considered when forming the box stiffness matrix. Due to the division of loading, correct deflections will result. In this manner the stiffness matrix for the box is found to be [Eq. (30a) used for rib stiffness]

$$[K]_{\text{box}} = \frac{Et}{2}\begin{array}{c} \begin{matrix} u_1 & v_1 & w_1 & u_2 & v_2 & w_2 \end{matrix} \\ \begin{bmatrix} 2.04782 & & & & & \\ -0.37500 & 1.52864 & & & & \\ -0.05227 & -0.00976 & 0.00430 & & & \\ -0.19329 & 0 & 0 & 2.04782 & & \\ 0 & -1.09515 & -0.00976 & 0.37500 & 1.52864 & \\ 0 & 0.00976 & -0.00098 & -0.05227 & 0.00976 & 0.00430 \end{bmatrix} \end{array} \tag{31}$$

The inverse of this matrix is the flexibility matrix.

$$[K]^{-1}_{\text{box}} = [C] = \frac{2}{Et}\begin{array}{c} \begin{matrix} F_{x_1} & F_{y_1} & F_{z_1} & F_{x_2} & F_{y_2} & F_{z_2} \end{matrix} \\ \begin{bmatrix} 0.81646 & & & & & \\ 0.22705 & 1.66224 & & & & \\ -10.47344 & 2.72965 & 409.39998 & & & \\ 0.20384 & -0.08123 & -5.55027 & 0.81646 & & \\ 0.08123 & 1.26026 & 5.01982 & -0.22705 & 1.66224 & \\ -5.55027 & -5.01982 & 142.67751 & -10.47344 & -2.72965 & 409.39998 \end{bmatrix} \end{array} \tag{32}$$

From the flexibility matrix, deflections due to applied loads can be found at once. For the two cases of applied loadings we find the following (rib treated as beam).

Case 1 (bending):

Forces of 1 lb. acting upward at each spar (nodes 1 and 2).

$$w_1 = 11{,}041.55/E \qquad u_1 = -320.47/E \qquad v_1 = -45.80/E$$
$$w_2 = 11{,}041.55/E \qquad u_2 = -320.47/E \qquad v_2 = 45.80/E$$

Case 2 (twisting):

Force of 1 lb. upward at node 1 and 1 lb. downward at node 2.

$$w_1 = 5{,}334.45/E \qquad u_1 = -98.46/E \qquad v_1 = 154.99/E$$
$$w_2 = -5{,}334.45/E \qquad u_2 = 98.46/E \qquad v_2 = 154.99/E$$

Similar results may be calculated for the case when the rib is assumed as a plate. Complete details are not given. In bending we get $w_1 = 10{,}888.12/E$, $u_1 = -310.56/E$, and $v_1 = -18.25/E$. Twisting results are $w_1 = 3615.72/E$, $u_1 = -25.84/E$, and $v_1 = 349.52/E$.

It is now advisable to select additional nodes and recalculate the previous deflection data. When added nodes have little effect on results, the process can be considered to have converged. Whether convergence be to the correct values requires additional information. These questions are now examined.

First, solutions are found for the node patterns shown in Fig. 16. Vertical deflections at node 1 for bending-type loading are as follows:

Fig. 16(a) $w_1 = 8558.0/E$

Fig. 16(b) $w_1 = 8591.2/E$

Fig. 16(c) $w_1 = 8548.4/E$

It is seen that the change in w_1 in going from the node pattern of Fig. 16(b) to 16(c) is about 1/2 per cent. Consequently convergence can be assumed to have been attained with the solution found from Fig. 16(b).

Obviously the first solution, based on Fig. 15, is in considerable error. This is due to the poor tie between spars and cover plate. Fig. 16(a) introduces an additional tie between these two components. The decreased value of w_1 for this case therefore reflects the added stiffness due to including the two nodes at the mid-span location.

An unexpected result is the close agreement between the solutions based on Figs. 16(a) and 16(b). In fact it would seem reasonable to expect Fig. 16(b) to lead to a smaller value for w_1 than that given by Fig. 16(a). Careful scrutiny, however, indicates that these results are quite reasonable. Whereas the node pattern of Fig. 16(b) accounts for shear lag in the cover plate, this is not the case with Fig. 16(a). As a result, the added stiffness in Fig. 16(b), due to the additional nodes connecting spars and cover skins, is offset by the added flexibility introduced by shear lag in cover skins. The results indicate these factors to be nearly equal; hence the reason for the nearly correct values given by Fig. 16(a).

Fig. 16(c) allows for shear lag and, at the same time, provides for adequate tie between spars and cover plates. It can therefore be felt that this node pattern will give final results which represent convergence of the method. As mentioned previously, this is substantiated by comparison with values obtained from Fig. 16(b).

There remains the question as to what is the correct value for w_1 for this problem. Elementary beam theory gives $w_1 = 6{,}900/E$, and, if extended to include shear distortion of spar webs, gives $w_1 = 7{,}740/E$. Using Reissner's shear lag theory,[13] the tip deflection is obtained as $w_1 = 7{,}900/E$. Finally if Reissner's shear lag theory is modified to include spar shear web deformation, the result is $w_1 = 8{,}740/E$. This is the most accurate theory available. It agrees to approximately 2 per cent with the numerical solution based on stiffness matrices.

The pronounced shear lag effect in this problem and its marked influence on the vertical tip deflection are significant. It is precisely this effect that produces a very complex stress distribution in the cover skins. Nevertheless the plate stiffness matrix developed in Eq. (27a) and based on triangular subelements represents this stress pattern with gratifying effectiveness.

The solution for the node pattern of Fig. 16(c) was obtained in a few minutes by utilizing a program for a high-speed digital computer that computed individual plate and spar stiffnesses and then combined these into the stiffness matrix for the complete box.

(XII) Reduction in Order of Stiffness Matrix

(1) *Eliminating Components of Node Displacement*

In an actual problem—as a wing analysis—the number of nodes to be used can become quite large. If, for purposes of discussion, 50 nodes are assumed, the stiffness matrix becomes of order 150 × 150. By eliminating u and v components of displacement at each node, the stiffness matrix can be reduced to order 50 × 50. However, this reduction process [see treatment of Eq. (23), for example] can require the calculation of the inverse of a 100 × 100 matrix. Such calculations are best avoided at present.

The problem that arises in eliminating the u and v components can be handled satisfactorily in any one of several ways. First, the calculation of the inverse of a large-order matrix can be avoided by eliminating a single component at a time. This is a practical expedient when automatic digital computing equipment

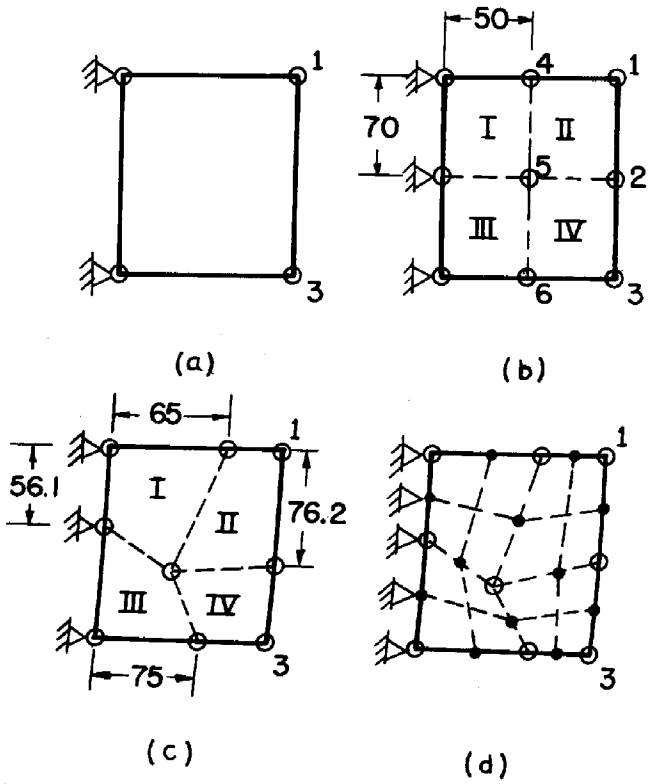

FIG. 13. Nodes and supports for clamped rectangular plate.

is available. Second, in some cases it may be feasible to eliminate "blocks" of u and v components at a time, thereby reducing the order of matrices to be inverted at any one time to a reasonable size (say 20×20). Third, the analysis can be carried out for sections of the structure, taken one by one. For each section, as a spanwise portion of the wing, the complete stiffness matrix can be determined. Elimination of u and v components can then be carried out at any selected nodes, except those common to two distinct sections of the structure. Each section can be treated in this manner. By properly adding the individual section stiffness matrices, the total stiffness matrix can be obtained. Finally u and v displacements at nodes where the sections join together can be eliminated. The stiffness matrix that remains will apply to w deflections only.

From a practical standpoint, the method just described has several worth-while features. For example all components of displacement at a given node may be eliminated. This can be useful when additional nodes are felt to be necessary in order to account properly for regions of maximum structural complexity. Even though eventually eliminated, these nodes will have contributed to the elements retained in the stiffness matrix.

(2) *Inversion of Stiffness Matrix*

Ordinarily, only the first few low-order vibration nodes and frequencies are required for the purpose of carrying out subsequent dynamic analyses. Using the stiffness matrix directly in the matrix iteration method leads to the highest frequency and corresponding mode. If the order of the stiffness matrix is high (say, 50×50), it becomes impractical to eliminate successively the higher modes and so eventually obtain the lowest modes.

Inversion of the stiffness matrix leads to the flexibility matrix. This matrix used in the matrix iteration procedure yields results for the lowest mode. Therefore, it is ordinarily preferable to know the flexibility matrix.

If the stiffness matrix is of high order (say, 50×50), inverting it becomes a major problem in itself. This can be overcome to some extent by employing the capabilities of present-day digital computing equipment. However, in many instances an alternative procedure may either be useful or necessary. Consequently, a possible approach to overcoming this difficulty will be outlined here.

The proposed method consists of converting the original stiffness matrix K into a lower order stiffness matrix K^*. This is accomplished by introducing a set of generalized coordinates which are related to the original displacements (on which K is based) through a set of appropriately chosen functions. The accuracy inherent in K will have a direct influence on K^*.

Suppose K is known for the cantilever beam of Fig. 17. The order of K is 10×10. Now assume a set of polynomials of the form

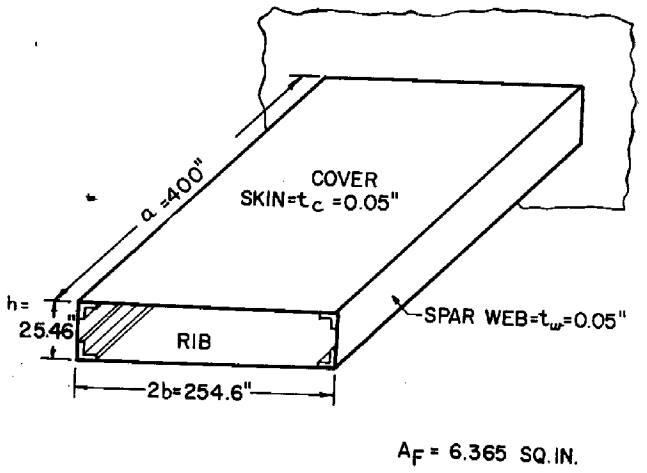

FIG. 14. Cantilevered box beam.

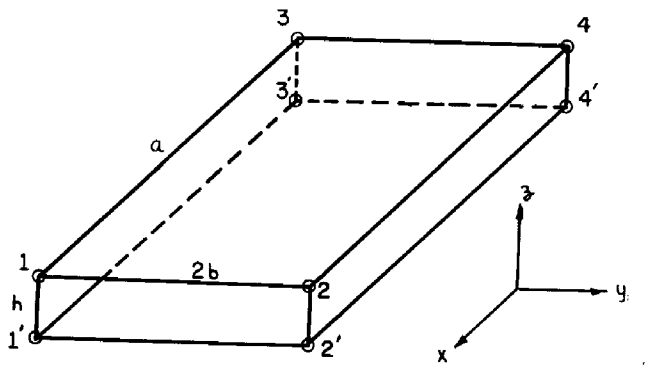

FIG. 15. Simplest node pattern for box beam.

$$\left.\begin{aligned} P_1(x) &= a_1x^2 + b_1x^3 + c_1x^4 \\ P_2(x) &= a_2x^2 + b_2x^3 + c_2x^5 \\ &\cdot \\ &\cdot \\ P_5(x) &= a_5x^2 + b_5x^3 + c_5x^8 \end{aligned}\right\} \tag{33}$$

Each of these will be made to satisfy the boundary conditions of the cantilever which are,

$$P_i(0) = P_i'(0) = P_i''(L) = P_i'''(L) = 0$$

Applying these conditions results in

$$\left.\begin{aligned} P_1(x) &= 6(x/L)^2 - 4(x/L)^3 + (x/L)^4 \\ P_2(x) &= 20(x/L)^2 - 10(x/L)^3 + (x/L)^5 \\ &\cdot \\ &\cdot \\ P_5(x) &= 140(x/L)^2 - 56(x/L)^3 + (x/L)^8 \end{aligned}\right\} \tag{34}$$

We now introduce generalized coordinates q_i which are related to the displacements y_i through the above polynomials. This relationship is established through the equations

$$\begin{Bmatrix} y_1 \\ y_2 \\ \cdot \\ \cdot \\ \cdot \\ \cdot \\ \cdot \\ \cdot \\ y_{10} \end{Bmatrix} = \begin{bmatrix} P_1(x_1) & P_2(x_1) & \cdot\ \cdot & P_5(x_1) \\ P_1(x_2) & P_2(x_2) & \cdot\ \cdot & P_5(x_2) \\ \cdot & & & \\ \cdot & & & \\ \cdot & & & \\ \cdot & & & \\ \cdot & & & \\ \cdot & & & \\ P_1(x_{10}) & P_2(x_{10}) & \cdot\ \cdot & P_5(x_{10}) \end{bmatrix} \begin{Bmatrix} q_1 \\ q_2 \\ q_3 \\ q_4 \\ q_5 \end{Bmatrix} \tag{35}$$

It is seen that the ten displacements $y_1, y_2, \ldots, y_{10}$ are to be replaced by the five coordinates $q_1, q_2, \ldots, q_5$.

The free vibration problem for the cantilever can be set up in terms of kinetic and potential energies. In terms of original displacements $y_1, y_2, \ldots, y_{10}$, these energies are, respectively,

$$\left.\begin{aligned} T &= (1/2)\,\{\dot{y}\}'\,[M]\,\{\dot{y}\} \quad \text{and} \\ V &= (1/2)\,\{y\}'\,[K]\,\{y\} \end{aligned}\right\} \tag{36}$$

where $[M]$ is the inertia (mass) matrix and $[K]$ the original 10×10 stiffness matrix.

Writing Eq. (35) as

$$\{y\} = [P]\,\{q\}$$

and substituting into Eqs. (36),

$$T = (1/2)\,\{\dot{q}\}'\,[P]'\,[M]\,[P]\,\{\dot{q}\}$$

$$V = (1/2)\,\{q\}'\,[P]'\,[K]\,[P]\,\{q\}$$

from which we define

$$\left.\begin{aligned} [K^*] &= [P]'\,[K]\,[P] \\ [M^*] &= [P]'\,[M]\,[P] \end{aligned}\right\} \tag{37}$$

If K is of order of 10×10 and P of order 10×5, K^* will be of order 5×5. The vibration analysis is now performed using K^* and M^*. By inverting K^* the lower modes can be calculated directly. Or alternatively, K^* can be used and all modes and frequencies determined, starting with the highest. This is feasible if K^* is of sufficiently low order (say, 10×10).

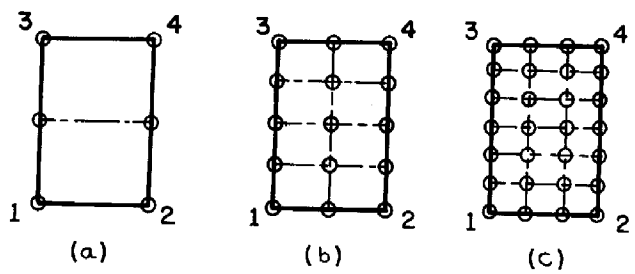

FIG. 16. Additional node patterns for box beam.

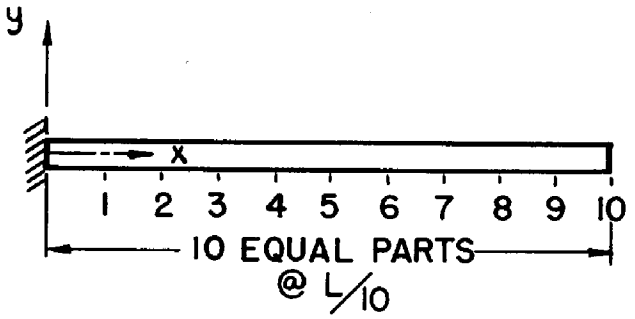

FIG. 17. Station selections on cantilever beam.

This process can be modified in several respects, and the purpose here is not to give an exhaustive treatment but rather to simply point out a possible approach to the problem. Preliminary calculations indicate that the idea may possess practical value. Extension to a two-dimensional grid can be made by generalizing the procedure suggested above.

APPENDIX (A)

DERIVATION OF SPAR STIFFNESS MATRIX

The structure and notation are described in Section (IX) and Fig. 4.

Flanges are assumed to carry axial stresses, while the web carries shear stresses. Cover plate material is not included as part of spar flanges. Derivation below is based on conventional beam theory.

Case 1

$u_1 = -u_1' \neq 0$; all other components of node displacement for the beam = 0.

The deflected beam and necessary forces and reactions are shown in Fig. A-1. Due to forces F_x at the left end, the beam deflects upward. The F_z forces cause a downward deflection. Beam theory, including effects of uniformly distributed shear in web, gives

$$w = \frac{F_{x_1}hL^2}{2EI} + \frac{2F_{z_1}L^3}{3EI}(1 + n) \tag{A-1}$$

$$\theta = \frac{F_{x_1}hL}{(EI)} + \frac{F_{z_1}L^2}{(EI)} \tag{A-2}$$

where w and θ are deflection and slope at the left end of

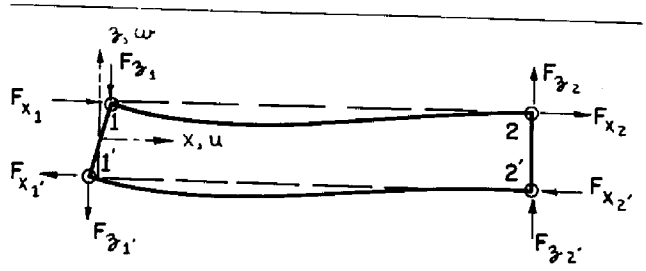

FIG. A-1. First beam displacement required in developing beam stiffness matrix.

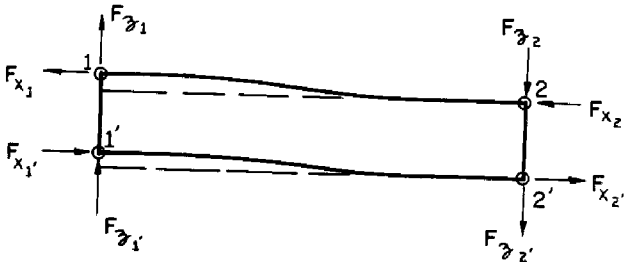

FIG. A-2. Second beam displacement required in developing beam stiffness matrix.

the beam, respectively, and n is given by Eq. (11b). Due to boundary conditions, $w = 0$; also, from the geometry of the deflected beam, $\theta = 2u_1/h$. Using these relations in Eqs. (A-1) and (A-2) and solving for forces gives

$$F_{x_1} = \frac{8EI}{h^2L}\frac{1+n}{1+4n}u_1 = \frac{6EI}{Lh^2(1+4n)}\frac{4}{3}(1+n)\,u_1 \tag{A-3}$$

$$F_{z_1} = -\frac{6EI}{hL^2}\frac{1}{1+4n}u_1 = -\frac{6EI}{Lh^2(1+4n)}\frac{h}{L}u_1 \tag{A-4}$$

Forces at node 2 follow from equilibrium considerations. They are

$$F_{x_2} = \frac{4EI}{h^2L}\frac{1-2n}{1+4n}u_1 = \frac{6EI}{Lh^2(1+4n)}\frac{2}{3}(1-2n)\,u_1 \tag{A-5}$$

$$F_{z_2} = -F_{z_1} \tag{A-6}$$

The above forces represent the first column of the required stiffness matrix. The other columns are found in a similar manner. When $w_1 = w_{1'} \neq 0$, while all other nodes are held fixed, the forces of Fig. A-2 apply.

Forces due to displacements imposed on the right-hand end of the beam may be written from the above results by analogy. The final spar stiffness matrix is given as Eq. (11a).

APPENDIX (B)

PLATE STIFFNESS MATRICES

Several plate stiffness matrices are given here without derivation.

(1) *Triangle—Arbitrary Node Locations*

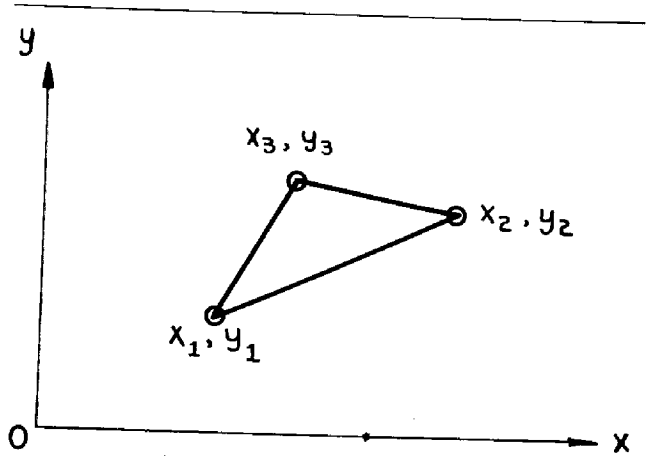

FIG. B-1. Triangular plate element with arbitrary node locations.

The stiffness matrix will be defined with respect to the equation

$$\begin{Bmatrix} F_{x_1} \\ F_{y_1} \\ F_{x_2} \\ F_{y_2} \\ F_{x_3} \\ F_{y_3} \end{Bmatrix} = [K] \begin{Bmatrix} u_1 \\ v_1 \\ u_2 \\ v_2 \\ u_3 \\ v_3 \end{Bmatrix} \tag{B-1}$$

Again adopting the notation

$$x_{ij} = x_i - x_j, \quad \lambda_1 = (1-\nu)/2, \quad \lambda_2 = (1+\nu)/2 \tag{B-2}$$

we get

$$[K] = \frac{Et}{2}\phi \begin{bmatrix} \lambda_1 x_{23}^2 + y_{23}^2 & & & & & \\ \lambda_2 x_{32}y_{23} & x_{23}^2 + \lambda_1 y_{23}^2 & & & & \\ \lambda_1 x_{23}x_{31} + y_{23}y_{31} & \lambda_1 x_{13}y_{23} + \nu x_{32}y_{31} & \lambda_1 x_{31}^2 + y_{31}^2 & & & \\ \lambda_1 x_{32}y_{31} + \nu x_{13}y_{23} & x_{23}x_{31} + \lambda_1 y_{23}y_{31} & \lambda_2 x_{13}y_{31} & x_{31}^2 + \lambda_1 y_{31}^2 & & \\ \lambda_1 x_{12}x_{23} + y_{12}y_{23} & \lambda_1 x_{21}y_{23} + \nu x_{32}y_{12} & \lambda_1 x_{12}x_{31} + y_{12}y_{31} & \lambda_1 x_{21}y_{31} + \nu x_{13}y_{12} & \lambda_1 x_{12}^2 + y_{12}^2 & \\ \lambda_1 x_{32}y_{12} + \nu x_{21}y_{23} & x_{12}x_{23} + \lambda_1 y_{12}y_{23} & \lambda_1 x_{13}y_{12} + \nu x_{21}y_{31} & x_{12}x_{31} + \lambda_1 y_{12}y_{31} & \lambda_2 x_{21}y_{12} & x_{12}^2 + \lambda_1 y_{12}^2 \end{bmatrix} \tag{B-3}$$

where

$$\phi = \frac{1/(1-\nu^2)}{x_{21}y_3 + x_{13}y_2 + x_{32}y_1}$$

(2) *Rectangle*

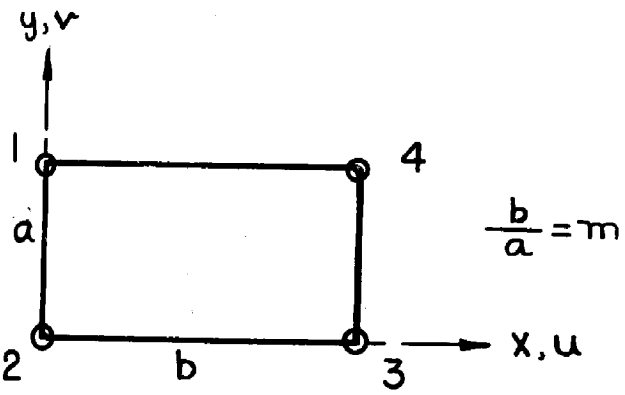

FIG. B-2. Node locations for rectangular plate element.

The stiffness matrix given below for the rectangle is based on the load states shown in Fig. 7. As a result this matrix is more general than that given in Eq. (27) due to the inclusion of linear terms in the strain expressions.

Again the stiffness matrix is arranged to agree with the equation

$$\begin{Bmatrix} F_{x_1} \\ F_{y_1} \\ F_{x_2} \\ F_{y_2} \\ F_{x_3} \\ F_{y_3} \\ F_{x_4} \\ F_{y_4} \end{Bmatrix} = [K] \begin{Bmatrix} u_1 \\ v_1 \\ u_2 \\ v_2 \\ u_3 \\ v_3 \\ u_4 \\ v_4 \end{Bmatrix} \tag{B-4}$$

in which $[K]$ is given by

$$[K] = \frac{Et}{8(1-\nu^2)} \begin{array}{c} \begin{matrix} u_1 & v_1 & u_2 & v_2 & u_3 & v_3 & u_4 & v_4 \end{matrix} \\ \begin{bmatrix} a_1+b_1 & & & & & & & \\ 1+\nu & a_2+b_2 & & & & & & \\ a_1-b_1 & 1-3\nu & a_1+b_1 & & & & & \\ 3\nu-1 & c_2-a_2 & -1-\nu & a_2+b_2 & & & & \\ -a_1-c_1 & -1-\nu & c_1-a_1 & 1-3\nu & a_1+b_1 & & & \\ -1-\nu & -a_2-c_2 & 3\nu-1 & a_2-b_2 & 1+\nu & a_2+b_2 & & \\ c_1-a_1 & 3\nu-1 & -a_1-c_1 & 1+\nu & a_1-b_1 & 1-3\nu & a_1+b_1 & \\ 1-3\nu & a_2-b_2 & 1+\nu & -a_2-c_2 & 3\nu-1 & c_2-a_2 & -1-\nu & a_2+b_2 \end{bmatrix} \end{array} \tag{B-5}$$

where, in the above matrix,

$$\left.\begin{array}{lll} a_1 = m(1-\nu), & b_1 = (2/3m)(4-\nu^2), & c_1 = (2/3m)(2+\nu^2) \\ a_2 = (1-\nu)/m, & b_2 = (2m/3)(4-\nu^2), & c_2 = (2m/3)(2+\nu^2) \end{array}\right\} \tag{B-6}$$

$$m = l/h \quad \text{(see Fig. 7)} \tag{B-7}$$

Eq. (B-5) simplifies to the following if $\nu = 1/3$:

$$[K] = \frac{Et}{96} \begin{array}{c} \begin{matrix} u_1 & v_1 & u_2 & v_2 & u_3 & v_3 & u_4 & v_4 \end{matrix} \\ \begin{bmatrix} \varphi_1(m) & & & & & & & \\ 18 & \varphi_1(1/m) & & & & & & \\ \varphi_2(m) & 0 & \varphi_1(m) & & & & & \\ 0 & \varphi_3(1/m) & -18 & \varphi_1(1/m) & & & & \\ \varphi_4(m) & -18 & \varphi_3(m) & 0 & \varphi_1(m) & & & \\ -18 & \varphi_4(1/m) & 0 & \varphi_2(1/m) & 18 & \varphi_1(1/m) & & \\ \varphi_3(m) & 0 & \varphi_4(m) & 18 & \varphi_2(m) & 0 & \varphi_1(m) & \\ 0 & \varphi_2(1/m) & 18 & \varphi_4(1/m) & 0 & \varphi_3(1/m) & -18 & \varphi_1(m) \end{bmatrix} \end{array} \tag{B-8}$$

where

$$\left.\begin{array}{lll} \varphi_1(m) = 9m + (35/m), & \varphi_1(1/m) = (9/m) + 35m \\ \varphi_2(m) = 9m - (35/m), & \varphi_2(1/m) = (9/m) - 35m \\ \varphi_3(m) = -9m + (19/m), & \varphi_3(1/m) = (-9/m) + 19m \\ \varphi_4(m) = -9m - (19/m), & \varphi_4(1/m) = (-9/m) - 19m \end{array}\right.$$

(3) *Other Shapes*

Although the parallelogram and arbitrary quadrilateral can be treated in a manner similar to that used for the rectangle, the individual elements in $[K]$ tend to become unwieldy. For that reason use of automatic digital computing equipment is considered to offer the practical means for obtaining stiffnesses of such plates. Programs for carrying out such calculations can be determined by following the basic ideas developed in this paper.

REFERENCES

[1] Schuerch, H. U., *Structural Analysis of Swept, Low Aspect Ratio, Multispar Aircraft Wings*, Aeronautical Engineering Review, Vol. 11, No. 11, p. 34, November, 1952.

(*Continued on page 854*)